Structural Engineering and Mechanics, *Vol. 65, No. 2 (2018) 163-171*
DOI: https://doi.org/10.12989/sem.2018.65.2.163

Effect of steel fiber volume fraction and aspect ratio type on the mechanical properties of SIFCON-based HPFRCC

Seugnwon Kim, Haekook Jung, Yongjae Kim and Cheolwoo Park*

Department of Civil Engineering, Kangwon National University, 346 Choongang-ro, Samcheok 25913, Republic of Korea

(Received December 15, 2017, Revised December 17, 2017, Accepted December 18, 2017)

Abstract. Plain concrete is a brittle material with a very low tensile strength compared to compressive strength and critical tensile strain. This study analyzed the dynamic characteristics of high-performance fiber-reinforced cementitious composites based on slurry-infiltrated fiber concrete (SIFCON-based HPFRCC), which maximizes the steel–fiber volume fraction and uses high-strength mortar to increase resistance to loads, such as explosion and impact, with a very short acting time. For major experimental variables, three levels of fiber aspect ratio and five levels of fiber volume fraction between 6.0% and 8.0% were considered, and the flexural strength and toughness characteristics were analyzed according to these variables. Furthermore, three levels of the aspect ratio of used steel fibers were considered. The highest flexural strength of 65.0 MPa was shown at the fiber aspect ratio of 80 and the fiber volume fraction of 7.0%, and the flexural strength and toughness increased proportionally to the fiber volume fraction. The test results according to fiber aspect ratio and fiber volume fraction revealed that after the initial crack, the load of the SIFCON-based HPFRCC continuously increased because of the high fiber volume fraction. In addition, sufficient residual strength was achieved after the maximum strength; this achievement will bring about positive effects on the brittle fracture of structures when an unexpected load, such as explosion or impact, is applied.

Keywords: SIFCON-based HPFRCC; flexural strength; flexural toughness; aspect ratio; steel-fiber volume fraction

1. Introduction

Plain concrete is a brittle material with a very low tensile strength compared to compressive strength and critical tensile strain. To prevent the brittle fracture of concrete material while improving the tensile behavior and energy dissipation capacity, high-performance fiber-reinforced cementitious composite (HPFRCC) has been actively researched in Korea and overseas (Ku *et al.* 2014, Kang 2013, Naaman *et al.* 2002, Banthia *et al*. 2007). In general, adding fibers to concrete can delay the initial crack generation and restrain the progress of cracks. Moreover, a large increase in strength and toughness can be expected (Lee and Yun 2010, Metha and Monreino 2006).

Furthermore, owing to the recent rapid development of construction technology, structures are becoming larger, higher, and longer, and the functions of structures are becoming more diversified and complicated, resulting in an increasing trend of unexpected loads, such as explosions and fires (Kim and Park 2016, Kim *et al.* 2014). In South Korea, where the concentration of population in large cities is inevitable, if structures are damaged because of loads, such as an explosion, collision or impact, their recovery is difficult, and there is a risk of damages occurring in a series.

The typical defense design to respond to unexpected loads in existing structures is to increase the thickness of the concrete wall. However, using high-performance materials, such as HPFRCC, provides advantages including improved utilization of structures and efficient reinforcement work (Park *et al.* 2016, Kim *et al.* 2015).

This study was conducted to analyze the dynamic characteristics of slurry-infiltrated fiber concrete (SIFCON) with maximum fiber volume and used high-strength mortar to increase resistance to loads with a very short acting time such as explosion and impact. For major experimental variables, the flexural strength and toughness were analyzed while changing the fiber volume fraction from 6.0% to 8.0% in 0.5% steps. In addition, three levels of the aspect ratios of steel fiber were considered.

2. Experimental details

2.1 Used materials

2.1.1 Cement

In this study, the type 1 ordinary Portland cement was used, the physical and chemical characteristics of which are listed in Table 1.

2.1.2 Silica fume

Silica fume was used as an admixture to manifest the high strength of the filling slurry; its physical and chemical characteristics are listed in Table 2.

2.1.3 Aggregate

Fine aggregates were used with 0.5 mm or smaller diameters produced by the J Company in South Korea to

*Corresponding author, Ph.D.
E-mail: tigerpark@kangwon.ac.kr

http://www.techno-press.com/journals/sem&subpage=7
ISSN: 1225-4568 (Print), 1598-6217 (Online)

Table 1 Material properties of ordinary Portland cement

Physical properties					
Specific gravity	Fineness (cm^2/g)	Stability (%)	Setting time(min)		LOI (%)
			Initial	Final	
3.15	3,400	0.10	230	410	2.58
Chemical compositions (%, mass)					
SiO_2	CaO	MgO	SO3	Al2O3	
21.95	60.12	3.32	2.11	6.59	

Table 2 Material properties of silica fume

Physical properties				
Specific gravity		Fineness (cm^2/g)		
2.10		200,000		
Chemical compositions (%, mass)				
SiO_2	CaO	MgO	SO_3	Al_2O_3
96.00	0.38	0.10	-	0.25

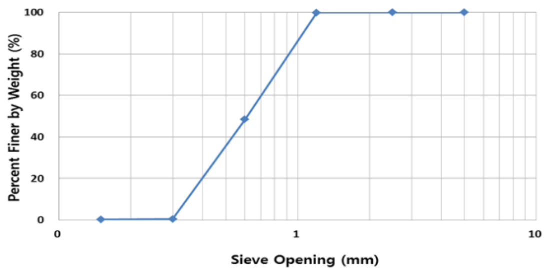

Fig. 1 Grading curve of fine aggregate

Table 3 Properties of polycarbonate-based high range water reducer

Principal component	Specific gravity	pH	Alkali content [%]	Chloride content [%]
Polycarboxylate	1.05± 0.05	5.0± 1.5	less than 0.01	less than 0.01

improve the filling performance of the slurry and reduce material separation. Furthermore, the ratio of the amount of fine aggregates to the binder was set at 1:0.5, and no coarse aggregates were used for filling between steel fibers. Fig. 1 shows the particle-size distribution of the fine aggregates used in this study.

2.1.4 High range water reducer (HRWR)

A polycarbonate-based high range water reducer, the properties of which are listed in Table 3, was used to improve the liquidity and filling performance of the slurry.

2.1.5 Steel fiber

The study used steel fibers for plain concrete with aspect ratios of 60 (diameter 0.5 mm, length 30 mm), 67 (diameter 0.9 mm, length 60 mm), and 80 (diameter 0.75 mm, length 60 mm). The tensile strength of steel fibers was 1,200 MPa. Fig. 2 shows the shape of the steel fibers used in this study.

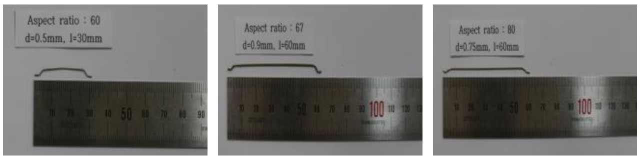

(a) Aspect ratio 60 (b) Aspect ratio 67 (c) Aspect ratio 80

Fig. 2 Types of steel fiber

Table 4 Mix proportions of mortar slurry

W/B ratio	0.4
Superplasticizer	2.5% (cement weight percent)
Fine aggregate content	1 : 0.5 (binder : fine aggregate)
Silica fume	15% (cement weight percent)

2.2 Mixing

For the mortar slurry to fill the inner space of steel fibers laid in advance, the water-binder ratio was fixed at 0.4 to provide the optimum charging performance through premixing, and the amount of high-performance water-reducing agent was set at 2.5% of the binder weight. In addition, to reduce material separation and achieve the required strength, the amounts of fine aggregates and silica fume corresponding to 0.5% and 15% of the binder cement weights, respectively, were replaced before mixing. Table 4 shows the mixing characteristics of the filling slurry used. The measured compressive strength of the filling slurry mortar in Table 4 was approximately 62 MPa (Kim *et al.* 2014).

In addition, flexure specimens with the five values of fiber volume fractions, that is, 6.0%, 6.5%, 7.0%, 7.5%, and 8.0% using steel fibers with the aspect ratios of 60, 67, and 80 were fabricated.

2.3 Experimental method

To evaluate the flexural performance of SIFCON-based HPFRCC according to the steel fiber volume fraction, prismatic specimens of 100 × 100 × 400 mm were fabricated in this study based on ASTM C 1609, and bending tests were conducted. As shown in Fig. 3, a 4-point force was applied using a 200-ton universal testing machine (UTM). In addition, the deflection displacement at the center was measured using a Japanese yoke, to which two linear variable differential transducers (LVDTs) were attached for the specimen center. The load was applied at the rate of 1 mm/min in the displacement control method. To evaluate the flexural performance, the flexural strength was calculated using Eq. (1) in ASTM C 1609.

$$F = \frac{PL}{bd^2} \tag{1}$$

where, P is the maximum load measured in the experiment, L is the span distance (300 mm), b is the specimen width (100 mm), and d is the specimen height (100 mm). To evaluate the energy absorption capacity according to the fiber volume fraction, the flexural toughness index was

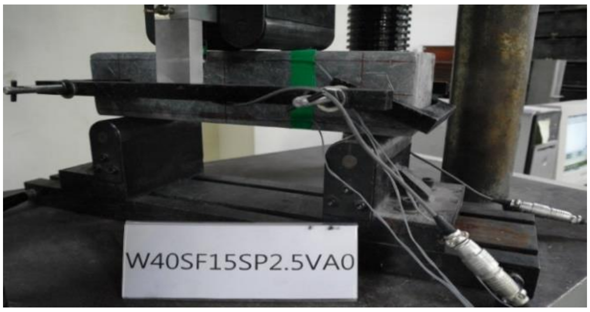

Fig. 3 Bending test with third-point loading

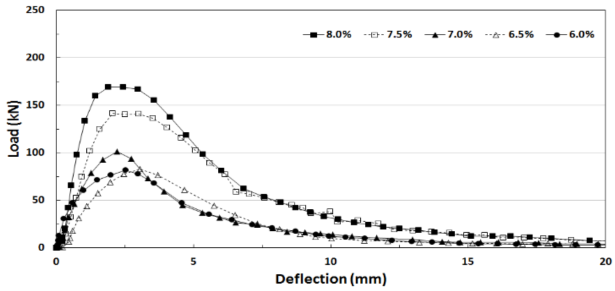

Fig. 4 Load-mid span deflection curves with respect to fiber volume fraction (aspect ratio 60)

calculated based on ASTM C 1609. However, it is inappropriate to define it as the area to 1/150 of the span distance L in the load-deflection curve, as suggested in ASTM C 1609, because of the flexural behavior characteristics of the SIFCON-based HPFRCC considered in this study. Therefore, to compare the energy absorption capacity according to the fiber volume fraction, the flexural toughness characteristics were instead analyzed using the area to 15 mm of deflection in the load-deflection curve.

3. Experiment results and analysis

3.1 Flexural behaviour characteristics

Figs. 4-6 show the load-deflection curves of each specimen according to the fiber aspect ratio and fiber volume fraction. The experimental results of flexural behavior characteristics according to the fiber aspect ratio and fiber volume fraction showed that the load of the SIFCON-based HPFRCC according to fiber volume fraction tended to continuously increase after the initial crack and reached the maximum load. Furthermore, the maximum load of every variable occurred at around 3 mm of the deflection regardless of the fiber volume fraction. This implies that the dynamic properties were improved so that the cement composites could resist loads, such as an impact, by absorbing sufficient energy even after the initial crack through the bridging of fibers according to high fiber volume fractions. Furthermore, the high strength of slurry matrix increased the bond strength with steel fibers, and the failure mode of fiber fracture at the fracture surface occurred along with the fiber-pulling phenomenon. Fig. 7 shows the final failure mode according to the fiber aspect ratio.

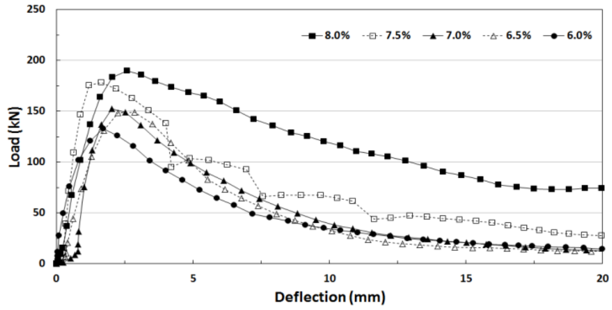

Fig. 5 Load-mid span deflection curves with respect to fiber volume fraction (aspect ratio 67)

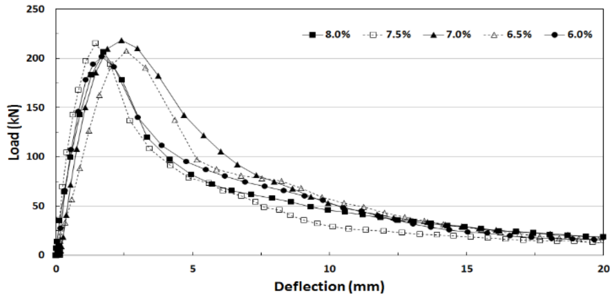

Fig. 6 Load-mid span deflection curves with respect to fiber volume fraction (aspect ratio 80)

(a) Aspect ratio 60 (b) Aspect ratio 67 (c) Aspect ratio 80

Fig. 7 High ductile behavior in bending test

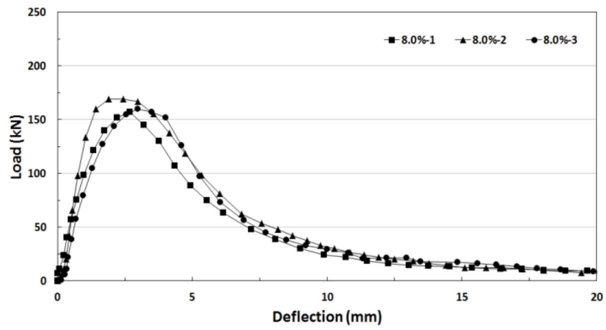

Fig. 8 Load-mid span deflection curve with 8.0% fiber volume fraction (aspect ratio 60)

Figs. 8-12 show the load–deflection curve according to the fiber volume fraction at the fiber aspect ratio of 60. The experimental result with a fiber volume fraction of 8.0% revealed a very excellent flexural resistance performance at the maximum load of 162.3 kN (flexural strength 48.6 MPa). In addition, the residual strength continued increasing after the maximum strength was reached. This suggests that when extreme loads, such as unexpected explosions and impacts, are applied, the collapse of structures due to brittle fracture can be prevented by obtaining additional residual strength.

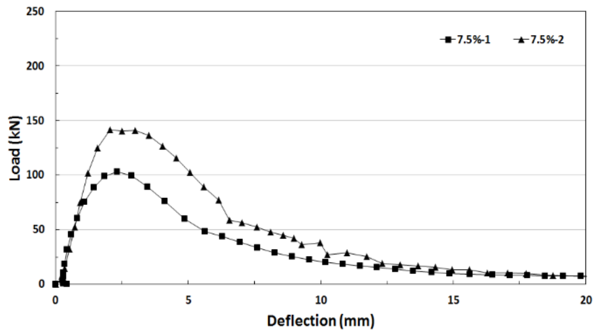

Fig. 9 Load-mid span deflection curve with 7.5% fiber volume fraction (aspect ratio 60)

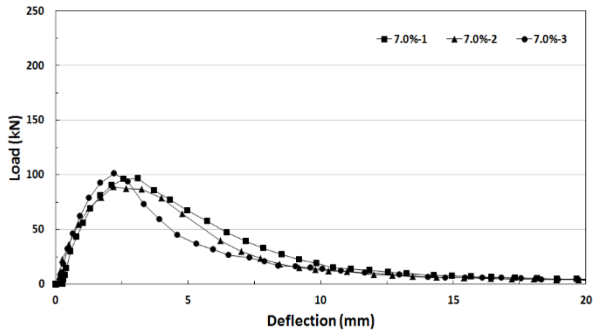

Fig. 10 Load-mid span deflection curve with 7.0% fiber volume fraction (aspect ratio 60)

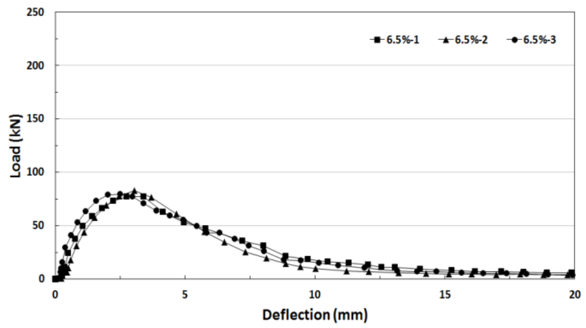

Fig. 11 Load-mid span deflection curve with 6.5% fiber volume fraction (aspect ratio 60)

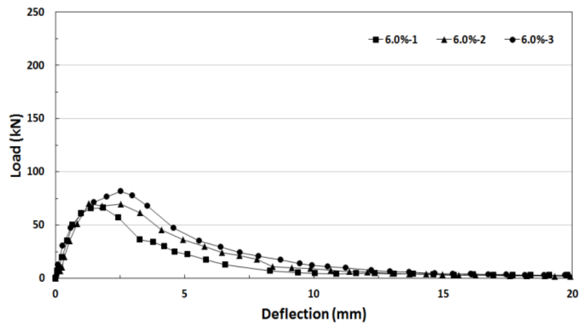

Fig. 12 Load-mid span deflection curve with 6.0% fiber volume fraction (aspect ratio 60)

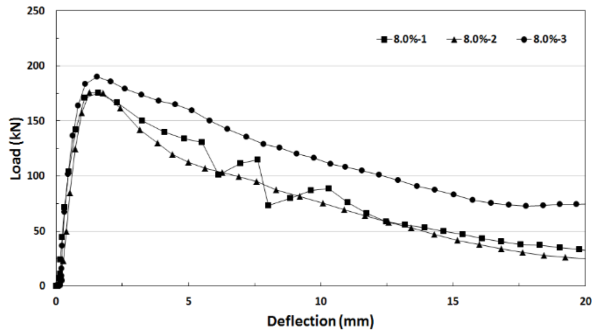

Fig. 13 Load-mid span deflection curve with 8.0% fiber volume fraction (aspect ratio 67)

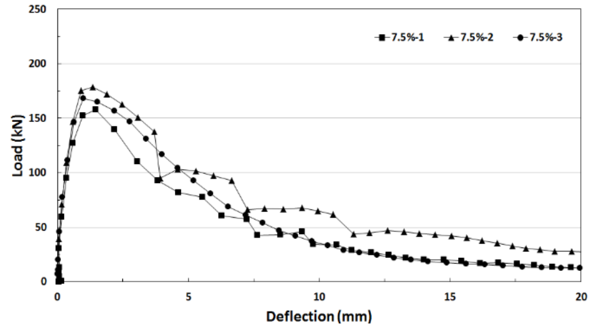

Fig. 14 Load-mid span deflection curve with 7.5% fiber volume fraction (aspect ratio 67)

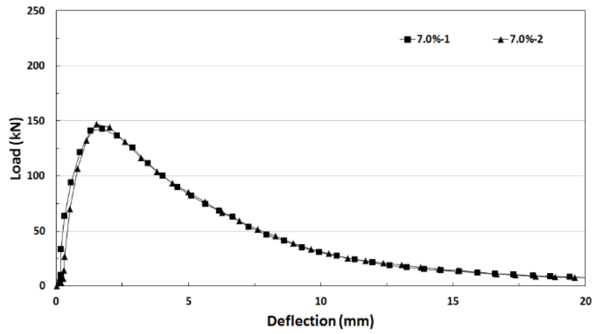

Fig. 15 Load-mid span deflection curve with 7.0% fiber volume fraction (aspect ratio 67)

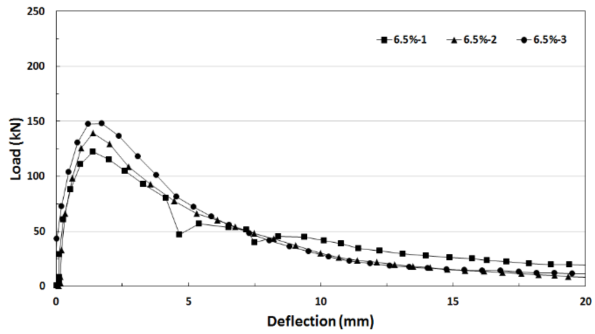

Fig. 16 Load-mid span deflection curve with 6.5% fiber volume fraction (aspect ratio 67)

The experimental results with fiber volume fractions of 7.5% and 7.0% showed maximum loads of 143.4 and 101.9 kN, respectively, which are approximately 88% and 61% of the maximum loads at the fiber volume fraction of 8.0%. Thus, the maximum load decreased with the decrease of fiber volume fraction. Accordingly, the flexural strength of steel fiber cement composites, with a high fiber volume fraction, was observed to sensitively decrease according to

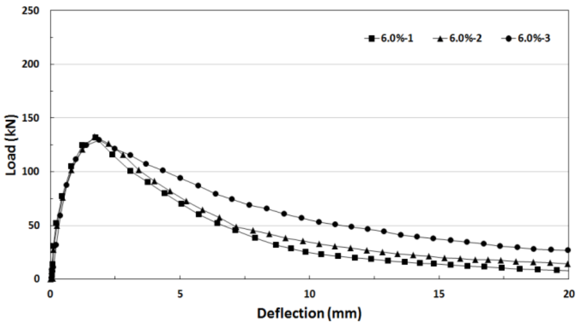

Fig. 17 Load-mid span deflection curve with 6.0% fiber volume fraction (aspect ratio 67)

the fiber density inside the specimen. Furthermore, the residual strengths at the fiber volume fractions of 8.0% and 7.5% after a certain deflection were similar. This suggests that the fiber density variation on the fracture section above a certain fiber volume fraction is insignificant and does not greatly affect the residual strength.

The experimental results with the fiber volume fractions of 6.5% and 6.0% showed approximately 50% and 46% of the maximum loads at the fiber volume fraction of 8.0%, respectively. The 0.5% difference in the fiber volume fractions of 6.5% and 6.0% caused no difference in the maximum load; however, the fiber volume fraction of 6.5% showed better residual strength after the maximum load was applied.

Figs. 13-17 show the load–deflection curves according to the fiber volume fraction at the fiber aspect ratio of 67. The experimental results with the fiber volume fractions of 8.0% showed the maximum load of 182.5 kN (flexural strength 54.8 MPa), which confirmed very excellent flexural resistance performance that is 13% higher than that at the fiber aspect ratio of 60. Furthermore, as with the fiber aspect ratio of 60, the residual strength continued increasing after the maximum strength was reached.

The experimental results with the fiber volume fractions of 7.5% and 7.0% showed maximum loads of 172.1 and 159.2 kN, respectively, which are approximately 94% and 87% of the maximum loads at the fiber volume fraction of 8.0%. Thus, the maximum load decreased with the decrease of fiber volume fraction, and the amount of decrement was smaller compared to that at the fiber aspect ratio of 60.

The experimental results with the fiber volume fractions of 6.5% and 6.0% showed maximum loads of approximately 77% and 72% of the maximum loads at the fiber volume fraction of 8.0%. The 0.5% difference in the fiber volume fractions of 6.5% and 6.0% caused no difference in the maximum load; however, the maximum load decreased distinctly below a certain level of fiber volume fraction.

Figs. 18-22 show the load–deflection curves according to the fiber volume fraction at the fiber aspect ratio of 80. The experimental results with the fiber volume fraction of 8.0% revealed very excellent flexural resistance performance with a maximum load of 204.0 kN (flexural strength of 61.2 MPa). This represents approximately 26% increase in the maximum load compared to the fiber aspect ratio of 60 at the fiber volume fraction of 8.0%.

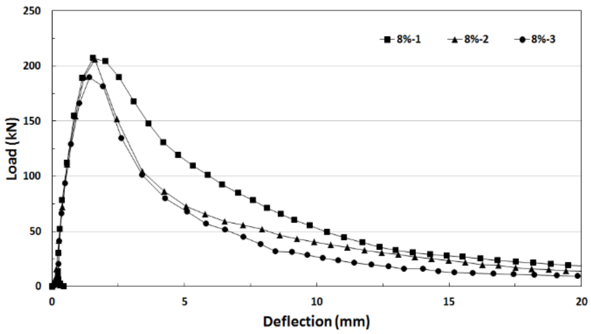

Fig. 18 Load-mid span deflection curve with 8.0% fiber volume fraction (aspect ratio 80)

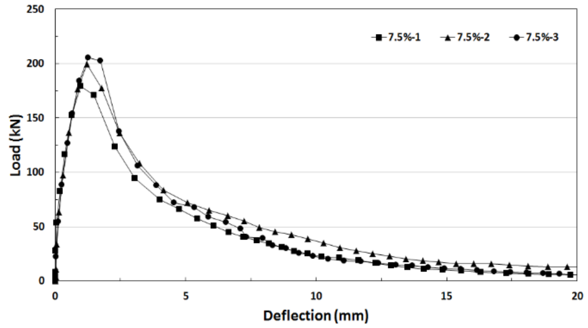

Fig. 19 Load-mid span deflection curve with 7.5% fiber volume fraction (aspect ratio 80)

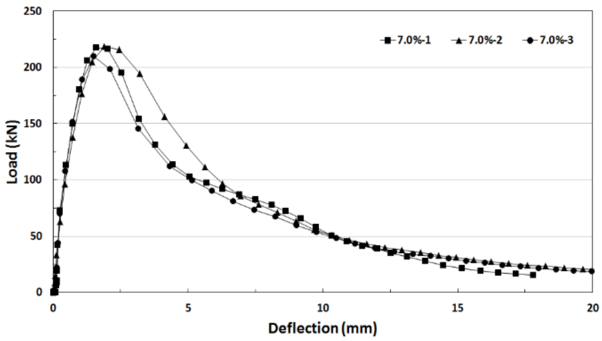

Fig. 20 Load-mid span deflection curve with 7.0% fiber volume fraction (aspect ratio 80)

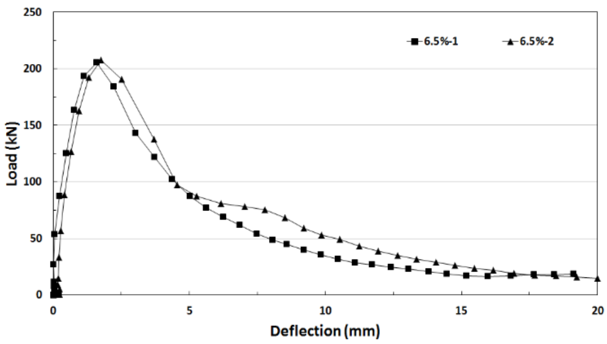

Fig. 21 Load-mid span deflection curve with 6.5% fiber volume fraction (aspect ratio 80)

Furthermore, the maximum load, which was 216.6 kN (flexural strength 65.0 MPa), at the fiber aspect ratio of 80 occurred at the fiber volume fraction of 7.0%.

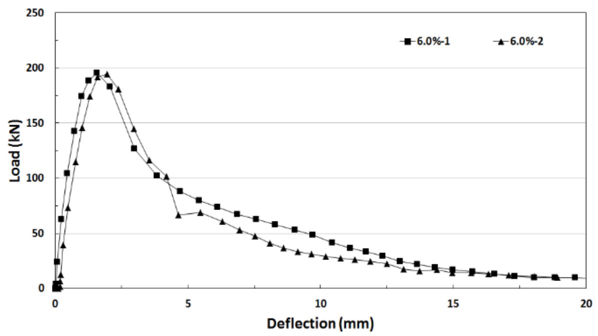

Fig. 22 Load-mid span deflection curve with 6.0% fiber volume fraction (aspect ratio 80)

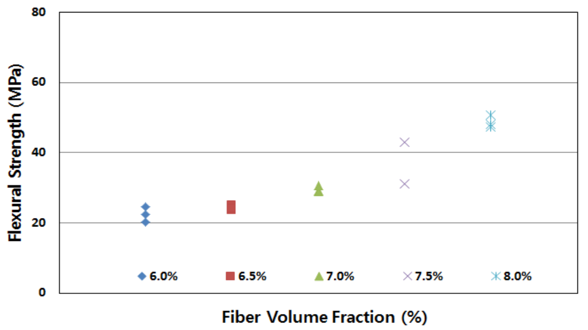

Fig. 23 Test results of flexural strength according to fiber volume fraction (aspect ratio 60)

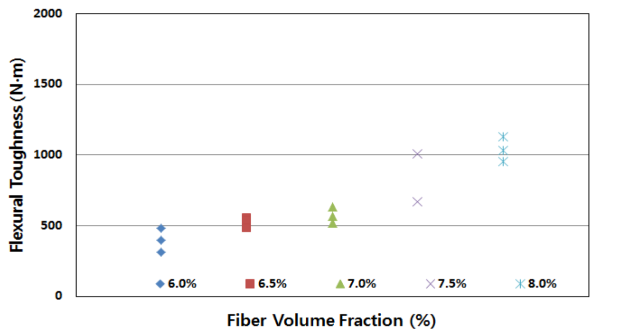

Fig. 24 Test results of flexural toughness according to fiber volume fraction (aspect ratio 60)

Table 5 Flexural strength and flexural toughness obtained from bending test (aspect ratio 60)

Variables (fiber volume fraction)	Flexural strength (MPa)	Flexural toughness (N·m)	Average of flexural strength (MPa)	Average of flexural toughness (N·m)
8.0%	47.2 50.8 48.1	48.7	951.3 1,125.7 1,031.1	1,036,0
7.5%	43.0 31.1	37.1	1,008.0 669.6	838.8
7.0%	29.2 28.9 30.6	29.6	630.0 566.6 518.0	571.5
6.5%	23.7 25.0 24.1	24.3	551.5 483.2 537.8	524.2
6.0%	20.1 22.3 24.5	22.3	311.1 398.2 480.5	396.6

Furthermore, the experimental results of the flexural resistance characteristics according to the fiber volume fraction showed the lowest maximum load of 200.0 kN (flexural strength 60.0 MPa) at the fiber volume fraction of 6.0%. This suggests that the increase in the flexural resistance performance according to the fiber volume fraction is insignificant.

As described above, owing to the high volume fraction of steel fibers, the specimens showed continuous load resistance with no sudden failure, indicating very excellent deformation capacity. Generally, after failure, the fiber volume fraction has a greater effect on the flexural toughness rather than on flexural strength. The results of the flexural behavior experiments according to fiber aspect ratio and fiber volume fraction revealed that an insignificant difference in flexural strength according to the fiber volume fraction at the fiber aspect ratio of 80. Although the load–deflection curves at the other fiber aspect ratios (60 and 67) were similar in general, the flexural strength showed distinct differences according to the fiber volume fraction. This could be because the composites of steel fibers and matrix showed homogeneous behaviors owing to the inclusion of relatively large number of fibers and high matrix strength due to the high volume fraction of steel fibers. Therefore, further research is needed on these flexural behavior characteristics according to the fiber aspect ratio.

3.2 Flexural strength and toughness

Fig. 23 compares the flexural strength experiment results according to the fiber volume fraction at the fiber aspect ratio of 60. The fiber volume fraction of 8.0% showed a high maximum flexural strength of 50 MPa. This suggests that it has very excellent resistance to bending unlike plain fiber-reinforced concrete. The maximum flexural strength at the fiber volume fraction of 7.5% was approximately 75% of that at the fiber volume fraction of 8.0%. The maximum flexural strength tended to decrease with the decrease in the fiber volume fraction.

This study attempted to analyze the flexural toughness characteristics based on ASTM C 1609; however, the flexural toughness index defined as the area to 1/150 of the span distance in the load-deflection curve, as suggested in ASTM C 1609, was inappropriate because the measured deflection greatly exceeded this value. Therefore, the flexural toughness was compared by the area to 15 mm of the deflection (span distance/20). Fig. 24 shows the flexural toughness according to the fiber volume fraction. The comparison of the flexural toughness until 15 mm of deflection showed an energy absorption capacity of approximately 381 Nm at the fiber volume fraction of 6.0%; however, the capacity was approximately 2.5 times higher, that is, 965 Nm, at the fiber volume fraction of 8.0%. The experimental results based on the fiber volume fraction revealed that the flexural toughness tended to increase with the fiber volume fraction, similar to the results of the flexural strength experiment. Table 5 outlines the calculation results of flexural strength and toughness according to the fiber volume fraction at the fiber aspect ratio of 60.

The mentioned analysis of flexural strength and

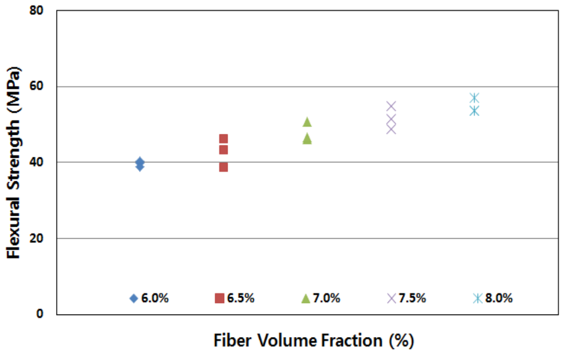

Fig. 25 Test results of flexural strength according to fiber volume fraction (aspect ratio 67)

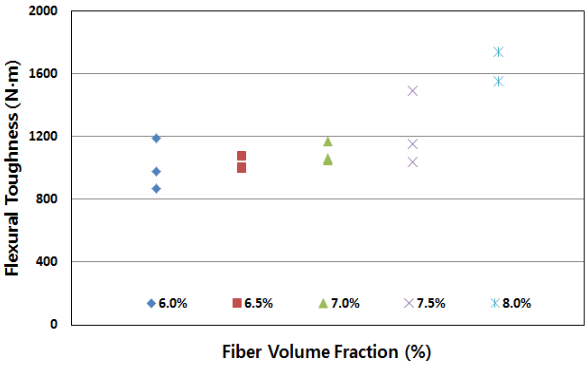

Fig. 26 Test results of flexural toughness according to fiber volume fraction (aspect ratio 67)

Table 6 Flexural strength and flexural toughness obtained from bending test (aspect ratio 67)

Variables (fiber volume fraction)	Flexural strength (MPa)	Flexural toughness (N·m)	Average of flexural strength (MPa)	Average of flexural toughness (N·m)
8.0%	53.5 53.7 57.1	1,736.5 1,550.8 2,295.8	54.8	1,861.0
7.5%	48.7 54.7 51.4	1,039.5 1,491.7 1,154.2	51.6	1,228.5
7.0%	46.1 46.5	1,052.3 1,061.5	47.8	1,056.9
6.5%	38.5 43.3 46.1	1,076.3 1,001.8 994.7	42.6	1,024.3
6.0%	40.4 38.9	975.9 1,186.5	39.7	1,009.3

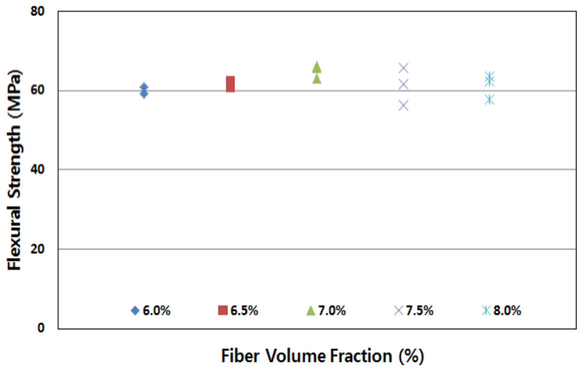

Fig. 27 Test results of flexural strength according to fiber volume fraction (aspect ratio 80)

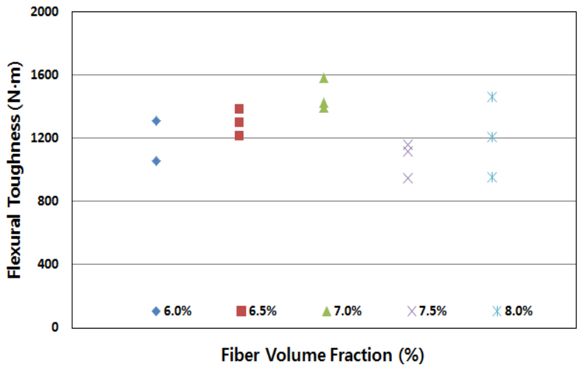

Fig. 28 Test results of flexural toughness according to fiber volume fraction (aspect ratio 80)

toughness show that the behavioral characteristics obtained from the experimental research slightly differ from the general tendency of the fiber volume fraction to greatly affect the fracture toughness after the initial crack or maximum load. This is because the combined action of the high fiber volume fraction and matrix strength of the cement composites in this study not only increased the fracture toughness but also greatly affected the flexural strength. Therefore, to achieve the performance required to increase resistance to impact or explosion loads, it will be advantageous to maintain the fiber volume fraction at the highest level through construction so as to increase flexural strength and toughness. However, this is limited to relatively small fibers with a diameter of 0.5 mm and length of 30 mm, as done in this study.

Fig. 25 compares the results of the flexural strength experiment conducted according to the fiber volume fraction at the fiber aspect ratio of 67. At the fiber volume fraction of 8.0%, the maximum flexural strength was approximately 55 MPa, which is an excellent flexural strength. The maximum flexural strengths at the fiber volume fractions of 7.5%, 7.0%, 6.5%, and 6.0% were approximately 94%, 87%, 78%, and 72% of that at the fiber volume fraction of 8.0%, respectively, indicating that the flexural strength also decreased with the decrease in fiber volume fraction.

Fig. 26 shows the flexural toughness according to the fiber volume fraction. The comparison of flexural toughness at the deflection of 15 mm revealed that the flexural toughness at the fiber volume fraction of 6.0% was approximately 1,010 Nm, which is 2.7 times higher than that at the fiber aspect ratio of 60 and fiber volume fraction of 6.0%. This implies that as the fiber length increased, the bond between steel fibers and slurry matrix increased; this in turn improved the energy absorption capacity. Furthermore, the fracture energy at the fiber volume fraction of 8.0% was 1,861 Nm, which is approximately 1.8 times higher than that at the fiber volume fraction of 6.0%, indicating a highly excellent energy absorption capacity. Similar to the results of the flexural strength experiment, the results of the flexural toughness experiment conducted according to the fiber volume fraction showed an increasing trend of flexural toughness according to the increase of fiber volume fraction. Table 6 outlines the calculation

Table 7 Flexural strength and flexural toughness obtained from bending test (aspect ratio 80)

Variables (fiber volume fraction)	Flexural strength (MPa)	Flexural toughness (N·m)	Average of flexural strength(MPa)	Average of flexural toughness(N·m)
8.0%	62.3 63.6 57.8	1,489.6 1,204.7 952.5	61.2	1,205.6
7.5%	56.3 61.5 65.6	945.6 1,161.7 1,115.3	61.1	1,074.2
7.0%	65.7 66.2 63.1	1,427.4 1,581.4 1,395.1	65.0	1,468.0
6.5%	61.6 62.4	1,214.5 1,381.3	62.0	1,297.9
6.0%	60.8 59.1	1,311.5 1,053.0	60.0	1,182.3

results of the maximum flexural strength and toughness according to the fiber volume fraction at the fiber aspect ratio of 67.

Fig. 27 compares the results of the flexural strength experiment according to the fiber volume fraction at the fiber aspect ratio of 80. The flexural strength at the fiber volume fraction of 7.0% was the best at every variable, and the maximum flexural strength was approximately 65 MPa. This is a very excellent flexural strength corresponding to approximately 75% of the compressive strength. The maximum flexural strengths at the fiber volume fractions of 8.0%, 7.5%, 6.5%, and 6.0% were 61.2, 61.1, 61.5, and 60.0 MPa, respectively. Thus, the excellent flexural strength values exceeding 60 MPa were obtained at every fiber volume fraction. The results of the flexural strength experiment according to the fiber volume fraction at the fiber aspect ratio of 80 revealed no difference in flexural strengths. This could be because the bond performance between the steel fibers and high-strength slurry matrix was improved when appropriate diameter and length of steel fibers were used. Based on this result, the actual application of the fiber aspect ratio of 80 will decrease the fiber volume fraction, and the dynamic performance will show no issues; this will enable economical construction.

Fig. 28 shows the flexural toughness according to the fiber volume fraction. The comparison of flexural toughness at a 15 mm deflection revealed a flexural toughness of approximately 1182 Nm at the fiber volume fraction of 6.0%. This flexural toughness was 3.1 and 1.2 times higher than the flexural toughness at the fiber volume fraction of 6.0% and fiber aspect ratios of 60 and 67, respectively. Furthermore, this result showed the highest energy absorption capacity of 1468 Nm at the fiber volume fraction of 7.0%, and this fracture energy was 1.3 times higher than the energy absorption capacity at the fiber volume fraction of 6.0%. Table 7 outlines the calculation results of the maximum flexural strength and toughness according to the fiber volume fraction at the fiber aspect ratio of 80.

5. Conclusions

In this study, the flexural behavior characteristics of SIFCON-based HPFRCC were analyzed according to the variations in fiber aspect ratio and fiber volume fraction to improve the resistance performance of concrete structures to unexpected loads such as explosion and impact. The following conclusions can be drawn from this study.

- The load of the SIFCON-based HPFRCC according to the fiber aspect ratio and fiber volume fraction continuously increased because of the high fiber volume fraction after the initial crack, and sufficient residual strength was obtained after the maximum strength. This sufficient residual strength is expected to bring about positive effects to the brittle fracture of structures when unexpected loads, such as explosion and impact, are applied.
- The maximum flexural strength at the fiber aspect ratio of 80 and fiber volume fraction of 7.0% was 65 MPa, which is a very excellent flexural resistance performance corresponding to approximately 75% of the compressive strength. In contrast, the maximum flexural strength at the fiber aspect ratio of 60 and fiber volume fraction of 6.0% was 22 MPa. Thus, a large difference was observed in the flexural strength according to the fiber aspect ratio and fiber volume fraction.
- The results of the flexural toughness and strength experiments showed a similar trend, and the fiber diameter and length greatly affected the energy absorption capacity. Furthermore, in the event of a fracture, the fibers also fractured and the fiber-pulling phenomenon occurred on the fracture surface. This suggests that the sufficiently high bond performance between the used steel fibers and slurry matrix increased the fracture energy.
- The shapes of the load-deflection curves plotted according to the fiber aspect ratio and fiber volume fraction were similar. However, all the fiber aspect ratios, except the ratio of 80, had a greater effect on the magnitude of flexural strength. This could be because the composites of steel fibers and matrix show homogeneous behaviors because a relatively large number of fibers were included owing to the various fiber diameters and lengths and the high fiber volume fraction; thus, the matrix strength increased.
- To meet the required performance for increasing resistance to explosion and impact loads, the energy absorption capacity will benefit in maintaining the fiber volume fraction at the highest level through constructions so as to increase flexural strength and toughness. Furthermore, the more economical use of steel fiber requires the determination of the fiber aspect ratio and volume fraction by reflecting the required characteristics of the structures against impact and explosion loads.

Acknowledgments

This research was supported by a grant (13SCIPA01) from Smart Civil Infrastructure Research Program funded by Ministry of Land, Infrastructure and Transport (MOLIT) of Korea government and Korea Agency for Infrastructure Technology Advancement (KAIA) and by a Construction Technology Research Project (17SCIP-B128706-01) funded by the Ministry of Land, Infrastructure and Transport, and this study was supported by 2015 Research Grant from Kangwon National University

References

ASTM C 1609 (2007), *Standard Test Method for Flexural Performance of Fiber-Reinforced Concrete (Using Beam with Third-Point Loading*, American Society for Testing and Materials (ASTM).

Banthia, N. and Sappakittipakorn, M. (2007), "Toughness enhancement in the steel fiber reinforced concrete through fibers hybridization", *Cement Concrete Res*., **37**(9), 1366-1372.

Park, C., Kim, Y., Choi, E. and Kim, S. (2016), "Fundamental properties and mechanical characteristics of high performance cement composite with steel fibers under high temperature", *J. Struct*. *Integr*. *Mainten*., **1**(4), 189-196.

Ku, D.O., Kim, S.D., Kim, H.S. and Choi, K.K. (2014), "Flexural performance characteristics of amorphous steel fiber-reinforced concrete", *J. Kor*. *Concrete Inst*., **26**(4), 483-489.

Kim, S.W., Jeon, S.P., Shin, S.M., Cho, H.M. and Park, C.W. (2014), "Evaluation on filling performance of high flow slurry with respect to quantity of fine aggregate", *Proceedings of the Korea Institute for Structural Maintenance and Inspection*, **18**(2), 407-409.

Metha, P.K. and Monreiro, P.J. (2006), *Concrete: Microstructure, Properties and Materials*, 3rd Edition, McGraw-Hill, Inc., New York.

Naaman, A.E. (2002), "Toughness, ductility, surface energy and deflection-hardening FRC composites", *Proceedings of the JCI International Workshop on Ductile Fiber-Reinforced Cementitious Composites (DRFCC)-Application and Evaluation (DFRCC-2002)*, 33-57.

Kim, S.W., Park, C.W., Kim, S.W., Cho, H.M., Jeon, S.P. and Ju, M.K. (2014), "Optimum mix proportions of in-fill slurry for high performance steel fiber reinforced cementitious composite", *J. Kor*. *Recycl*. *Constr*. *Res*. *Inst*., **2**(3), 196-201.

Kim, S.W., Cho, H.M., Lee, H.Y. and Park, C.W. (2015), "Flexural performance characteristics of high performance slurry infiltrated fiber reinforced cementitious composite according to volume fraction", *J. Kor*. *Inst*. *Struct*. *Mainten*. *Inspect*., **19**(4), 109-115.

Kim, S. and Park, C. (2016), "Flexural behavior of high-volume steel fiber cementitious composite externally reinforced with basalt FRP sheet", *J. Eng*., **2016**, 1-9.

Kang, S.T. (2013), "Bond strength of steel fiber incorporated in ultra high performance fiber-reinforced concrete", *J. Kor*. *Concrete Inst*., **25**(5), 547-554.

Lee, Y.O. and Yun, H.D. (2010), "Effects of expansive admixture on the mechanical properties of strain-hardening cement composite (SHCC)", *J. Kor*. *Concrete Inst*., **22**(5), 617-624.

CC